Vibrational Spectroscopy

Vibrational Spectroscopy of the Dehydrogenated Uracil Radical by Autodetachment of Dipole-Bound Excited States of Cold Anions**

Hong-Tao Liu, Chuan-Gang Ning, Dao-Ling Huang, and Lai-Sheng Wang

Abstract: *Molecules with large enough dipole moments can bind an electron by the dipole field, which has little effect on the molecular core. A molecular anion can be excited to a dipole-bound state, which can autodetach by vibronic coupling. Autodetachment spectroscopy of a complex anion cooled in a cryogenic ion trap is reported. Vibrational spectroscopy of the dehydrogenated uracil radical is obtained by a dipole-bound state with partial rotational resolution. Fundamental frequencies for 21 vibrational modes of the uracil radical are reported. The electron affinity of the uracil radical is measured accurately to be 3.4810 ± 0.0006 eV and the binding energy of the dipole-bound state is measured to be 146 ± 5 cm^{-1}. The rotational temperature of the trapped uracil anion is evaluated to be 35 K.*

High-resolution vibrational spectroscopy of transient species is important for determining their molecular structures and understanding their chemical reactivity. However, the low abundance and high reactivity of molecular radicals pose major challenges to conventional absorption spectroscopic methods.[1,2] Matrix isolation infrared spectroscopy can probe the vibrational structure of transient species trapped in low-temperature matrices, but the measured vibrational frequencies have matrix shifts.[3,4] Velocity modulation spectroscopy is a powerful tool to probing vibrational spectroscopy of molecular ions in hot plasmas,[5] but only the most abundant ions in the plasma environment can be studied.[6] Cavity-ring-down spectroscopy is one of the most sensitive optical spectroscopic methods,[7,8] but the sensitivity is still too low for single-molecule detection.[9] Infrared photodissociation action spectroscopy takes full advantage of the ultrahigh sensitivity of ion detection and has been used to determine the structures of many molecular ions.[10–14] This method was initially focused on molecular ions, and has been extended to the study of neutral clusters using IR/UV two-color photo-

ionization,[15,16] but the study of transient molecular radical species is still relatively rare.[17]

Autodetachment spectroscopy of molecular anions has high sensitivity for the detection of electrons, and its resolution was not limited by the electron energy analyzers.[18,19] Negative ions with sufficient binding energies can support electronically excited states, which was first observed in C$_2^-$.[20] By tuning the laser wavelength near the photodetachment threshold, resonant absorptions may be observed. If the total energy of the excited anion is above the electron detachment continuum, an electron may spontaneously escape from the anion (autodetachment).[21] In this case, ultrahigh optical resolution can be achieved by monitoring the total electron yield as a function of the photon energy.[19] Negative ions with electronically excited states are not common, because of the low electron binding energies encountered for most anions. On the other hand, if the binding energy of an anion is lower than its vibrational energy, such as the case in NH$^-$, autodetachment can be realized through vibrational excitation within the ground electronic state.[22–25] This technique is limited to anions with sufficiently low electron binding energies. The observation of dipole-bound excited state in anions[26,27] extends autodetachment spectroscopy to more molecular anions, if the corresponding neutral radicals possess a large enough dipole moment (> 2.5 D).[28–30] Ultrahigh resolution spectroscopy of dipole-bound states (DBS) has been demonstrated.[31,32] However, there have been only a limited number of autodetachment spectra of DBS reported over the past three decades. The difficulty of assigning the congested spectra at room temperature hinders its more extensive application, in particular to more complex molecular species.[32]

We have developed an cryogenically controlled ion trap, coupled to a magnetic-bottle photoelectron analyzer,[33–35] which can completely eliminate vibrational hot bands in photoelectron spectra of molecular anions. Recently, we have built an improved version of the cryogenic ion trap[36] coupled with high-resolution photoelectron imaging.[37,38] Our initial experiments on cold phenoxide anions have shown that not only vibrational hot bands were completely suppressed, but a rotational profile was also observed.[39] More significantly, we observed DBS resonances, which allowed a number of vibrational modes with very weak Frank–Condon factors to be "lightened" up by vibrational autodetachment.[39] The vibrational frequencies of the DBS were found to be the same as those of the neutral radical, suggesting that vibrational structures of dipolar radicals can be probed by DBS. Here we report the first high-resolution vibrational spectroscopy study of the dehydrogenated uracil radical, with partial rotational resolution, by autodetachment from DBS of cold deproton-

[*] Dr. H. T. Liu, D. L. Huang, Prof. Dr. L. S. Wang
Department of Chemistry, Brown University
Providence, RI 02912 (USA)
E-mail: Lai-Sheng_Wang@brown.edu

Prof. Dr. C. G. Ning
Department of Physics
State Key Laboratory of Low-Dimensional Quantum Physics
Tsinghua University, Beijing, 100084 (China)
and
Collaborative Innovation Center of Quantum Matter
Beijing (China)

ated uracil anions. Rich vibrational information is obtained for this important radical species. More interestingly, the resolved rotational profiles allow us to characterize the rotational temperature of the trapped anions for the first time.

The dehydrogenated uracil radical ([U-H]·) is important in the chemistry of radiation damage in living cells.[40–42] The parent uracil molecule can form a "ground-state" dipole-bound anion, which has been studied by both Rydberg electron transfer and photoelectron spectroscopy.[43–45] We expect the dehydrogenated [U-H]· radical to possess a large dipole moment to support a DBS. Scheme 1 shows the two [U-H]· radical isomers with dehydrogenation from the two
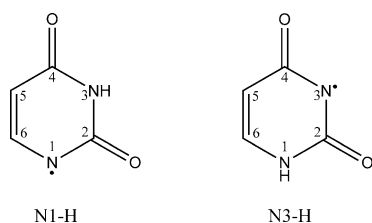
Scheme 1. Structures of the two stable deprotonated uracil radical isomers: [N1-H]· (left) and [N3-H]· (right).

different N sites (named as [N1-H]· and [N3-H]· for convenience in the following discussion). The electron affinities (EAs) of the [N1-H]· and [N3-H]· radicals have been calculated to be 3.4 and 3.8 eV, respectively.[46–48] Thus far, neither the EAs nor the vibrational structures of the [U-H]· radicals are known experimentally.

In the current study, the deprotonated uracil anions [U-H]⁻ were produced by electrospray of a mixed uracil/sodium hydroxide water/methanol (1:9 ratio) solution (pH about 8).[49] Anions from the electrospray source were transported into a temperature-controlled ion trap, where they were accumulated and cooled for 0.1 s before being ejected into the extraction zone of a time-of-flight mass spectrometer.[39] A dye laser with a tunable wavelength in the UV range ($\Delta\lambda$ about 0.0015 nm, Sirah Cobra-Stretch with a frequency doubling unit) was used for photodetachment. The laser wavelength was monitored by a wavelength meter ($\Delta\lambda$ about 0.001 nm, Bristol model 821), and the photoelectron imaging spectrometer was calibrated using the known spectra of Au⁻.[50] More experi-

mental details are given in the Supporting Informaiton.

Figure 1 shows the total electron yield from [U-H]⁻ as a function of the detachment laser wavelength with a scanning range of 1850 cm⁻¹ near and above the photodetachment threshold. The sharp peaks are due to autodetachment from the vibrational levels of the DBS of [U-H]⁻, as schematically shown in Figure S1. The very weak peak at $h\nu = 27\,930$ cm⁻¹ (label as "*" in the tenfold enlarged inset) is the transition from the anion ground state to the lowest vibrational state of the DBS (0←0 transition), as a result of resonant two-photon detachment.[39] The EA of the [U-H]· radical is determined as $28\,076 \pm 5$ cm⁻¹ (3.4810 ± 0.0006 eV), which is the onset of the direct nonresonant one-photon photodetachment from [U-H]⁻, as indicated by the arrow. Clearly, the autodetachment is much more intense relative to the nonresonant detachment process. The binding energy of the DBS of [U-H]⁻ is measured as 146 ± 5 cm⁻¹, which is the difference between the EA of the neutral [U-H]· radical and the excitation energy to the DBS vibrational ground state. The scale of the bottom axis in Figure 1 is the photon energy ($h\nu$), and the origin of the top scale refers to the 0←0 transition to the DBS. Hence all the vibrational excitations of the DBS can be directly read off the top axis. A total of 46 vibrational autodetachment resonances were observed; their energies and assignments are given in Table S1. The observed transitions consisted of vibrational fundamentals, overtones, and combination bands of the DBS. The assignments are based on the photoelectron spectra recorded for each vibrational resonance and the vibrational autodetachment propensity rule ($\Delta\nu = -1$) between the vibrational level of the DBS and the neutral final state (Figure S1).[51–53] The high resolution photoelectron spectra are extremely helpful for the vibrational assignments, as shown recently for the case of the phenoxide anion.[39] This is an important advantage of the current technique, compared
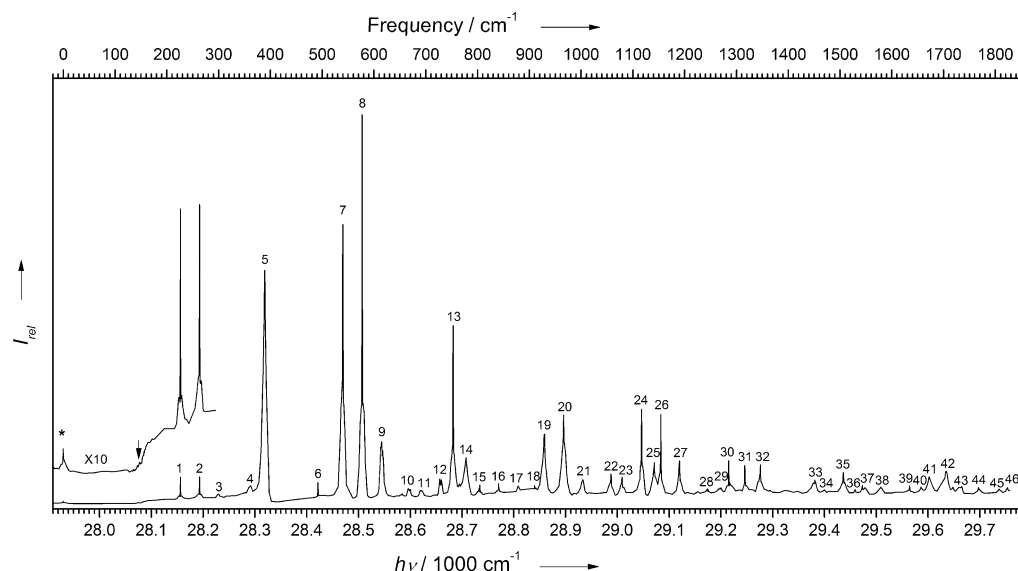

Figure 1. Autodetachment spectrum of deprotonated uracil anions ([N1-H]⁻) by measuring the total electron yield as a function of laser wavelengths across the detachment threshold. In the ×10 insert, the weak peak (label as *) at $h\nu = 27\,930$ cm⁻¹ represents the dipole-bound ground state; the electron signals came from resonant two-photon detachment. The arrow indicates the detachment threshold of the [N1-H]⁻ anion, measured as $28\,076 \pm 5$ cm⁻¹. See the text for details.

with previous autodetachment spectroscopy studies,[31,32] where the energy spectra of the autodetached electrons were not recorded. More importantly, the cold anions in the current work eliminated vibrational hot bands and significantly reduced rotational broadening, which greatly simplified the observed autodetachment spectrum in Figure 1. All the observed fundamental vibrational modes for the DBS (or the neutral [U-H]• radical) are given in Table 1. We are able to

Table 1: Experimental and theoretical vibrational frequencies (in cm^{-1}) of dehydrogenated uracil radical ([N1-H]•). Harmonic frequencies are calculated with B3LYP/6-311+ +G** method.

Mode	Symmetry	Theoretical ν	Experimental ν	Peak
ν_1	A′	3581		
ν_2		3222		
ν_3		3145		
ν_4		1713	1705	42
ν_5		1694	1672	41
ν_6		1469	1451	33
ν_7		1437		
ν_8		1411		
ν_9		1342	1316	31
ν_{10}		1301	1285	30
ν_{11}		1186	1154	26
ν_{12}		1082	1057	22
ν_{13}		982	970[a]	20
ν_{14}		920	910	18
ν_{15}		757	753	13
ν_{16}		583	577	8
ν_{17}		545	540	7
ν_{18}		501	492	6
ν_{19}		392	389	5
ν_{20}	A″	980		
ν_{21}		803	804	15
ν_{22}		734	727	12
ν_{23}		684	666	10
ν_{24}		633	615	9
ν_{25}		357	360	4
ν_{26}		152	150[b]	
ν_{27}		113	113[c]	

[a] The calculated frequencies of ν_{13} and ν_{20} are similar. The assignment of the 970 cm^{-1} resonance to ν_{13} is based on the observed *c*-type rotational profile. [b] ν_{26} can be obtained from either the overtone at 300 cm^{-1} (peak 3) or the $\nu_{26}+\nu_{27}$ combination band at 263 cm^{-1} (peak 2). [c] ν_{27} was obtained from its overtone at 226 cm^{-1} (peak 1).

obtain fundamental vibrational frequencies for 21 vibrational modes of the U-H radical out of a total of 27 possible modes.

The dipole-bound electron is weakly attracted by the positive end of the dipole, and it has little effect on the neutral core.[39] Therefore, the measured vibrational frequencies of the DBS can be taken as the vibrational frequencies of the neutral [U-H]• radical. In Table 1, the measured vibrational frequencies are compared with the calculated frequencies of the [N1-H]• isomer of the [U-H]• radical (Scheme 1). The calculations were done with the B3LYP/6-311++G** method using Gaussian 09 (see the Supporting Information).[54–57] The agreement between the observed and computed frequencies (unscaled) is excellent, suggesting that only the [N1-H]• isomer was probed in the experiment. The

measured detachment threshold of 3.4810 ± 0.0006 eV is also in good agreement with the calculated EA of the [N1-H]• radical (3.4 eV).[47] The EA of the [N3-H]• isomer was predicted to be about 3.8 eV,[47] which would be beyond the photon energy range (3.45–3.69 eV) covered in the current study (Figure 1). In addition, the [N3-H]⁻ anion was calculated to be about 0.5 eV higher in energy than the [N1-H]⁻ isomer[47,58] and hence was not expected to be populated in our low-temperature ion trap. We should also point out that only the lowest energy isomer was observed in a previous study of deprotonated thymine and cytosine anions.[59]

The [N1-H]• radical has a planar structure with C_s symmetry. Among its 27 normal modes of vibration (Table 1 and Figure S2), 19 are in-plane vibrations with A′ symmetry, and 8 are out-of-plane with A″ symmetry. In conventional photoelectron spectroscopy, the accessible vibrational excitations are limited to the Franck–Condon-active and totally symmetric modes. Usually very few such modes are observable in high-resolution photoelectron spectroscopy. Most vibrational modes are either not Franck–Condon-active or too weak to be clearly resolved. Surprisingly, 21 vibrational modes of the [N1-H]⁻ DBS were observed (Figure S1 and Table 1). Even more surprising, all the out-of-plane modes except one (ν_{20} in Table 1) were observed. This was most likely due to strong vibronic couplings and/or it might indicate the neutral radical is not truly planar or very floppy.

Rotational profiles were observed for most of the autodetachment peaks in Figure 1 and different rotational profiles were observed for the in-plane and out-of-plane vibrational peaks. Transitions to the in-plane vibrational modes with A′ symmetry exhibit *c*-type rotational contours, while transitions to the out-of-plane vibrational modes with A″ symmetry exhibit *b*-type rotational contours, as shown in Figure 2 for the ν_{16} (*c*-type) and ν_{24} (*b*-type) modes. The *c*-type bands are dominated by a narrow Q branch with relatively small intensities from the P and R branches, whereas the *b*-type bands appear broad with the Q branch overlapped with the P branch at similar intensities. The two different rotational profiles for the ν_{16} and ν_{24} bands were simulated using the PGOPHER program[60] and compared with the experimental data in Figure 2. The simulation used calculated rotational parameters (see the Supporting Information) and yielded $J_{max} = 50$ and $T_{rot} = 35$ K. The spectral width used was 0.4 cm^{-1} for ν_{16} and 1.2 cm^{-1} for ν_{24}. The 0.4 cm^{-1} spectral width for mode ν_{16} is comparable to the fine step size (0.005 nm) of the dye laser used to obtain the spectrum in Figure 2. The broader spectral width for mode ν_{24} indicating a much faster autodetachment rate, and the 1.2 cm^{-1} spectral width is mainly due to lifetime broadening (approximately 4.4 ps).[32] Autodetachment rates for rovibrational excitation levels of DBS are determined primarily by vibrational motion of the neutral core, and vibration-induced dipole moment changes were believed to be the dominant effect governing the autodetachment rate.[32] The calculated IR intensity of mode ν_{24} is also much greater than that of mode ν_{16}, suggesting mode ν_{24} involves a much greater dipole moment change.

The rotational temperature that we obtained from the PGOPHER simulation is very important because it is
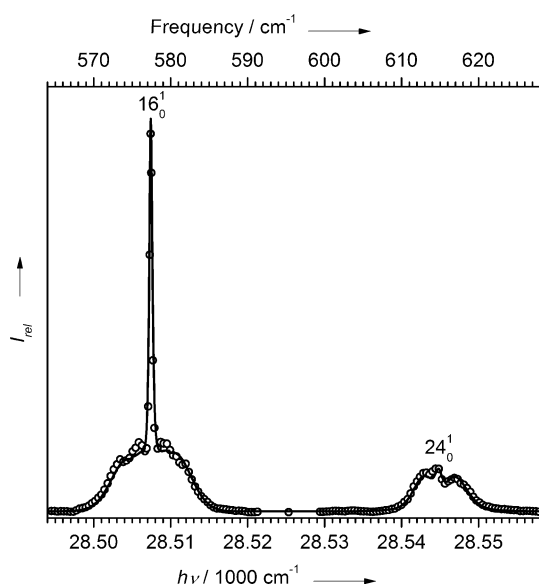
Figure 2. Comparison of observed and simulated spectra of ν_{16} (577 cm^{-1}, *c*-type) and ν_{24} (615 cm^{-1}, *b*-type) in the frequency region of 564 to 628 cm^{-1} with a resolution of 0.4 cm^{-1}. The circles are the experimental data and the solid line is the simulation ($J_{max}=50$, and $T_{rot}=35$ K). The simulated spectral width is 0.4 cm^{-1} for ν_{16} and 1.2 cm^{-1} for ν_{24}.

generally not known for cryogenically cooled ionic species. In the current experiment, the ion trap is attached to a cryogenic cold head operated at 4.4 K. The trapped [N1-H]$^-$ anions were cooled by collisions with the He/H$_2$ buffer gases for about 0.1 second. Although it is believed the [N1-H]$^-$ anions were in thermal equilibrium with the buffer gas, the exact temperature of the trapped anions was not known. The 35 K rotational temperature obtained for the [N1-H]$^-$ anions suggested that either the anions were not completely equilibrated rotationally or it could be heated possibly because of collisions with the background gas during the ion extraction process, which involved an acceleration of the anions by a 15 V extraction potential.

In summary, we report for the first time high-resolution vibrational spectroscopy of the dehydrogenated uracil radical. Fundamental vibrational frequencies of 21 normal modes out of a total of 27 were accurately measured by autodetachment from DBS of cold deprotonated [N1-H]$^-$ anions. The EA of the [N1-H]$^\bullet$ radical was determined to be 3.4810 ± 0.0006 eV. The well-resolved rotational profiles provide extra information of the trapped anion temperature. The current study provides a new approach to obtain high-resolution vibrational spectroscopy of transient dipolar radicals by autodetachment of DBS of cold anions. The current approach has a few unique advantages. First, resonant excitations to dipole-bound states usually occur in the visible or UV regime. Thus, vibrational spectroscopy for dipolar radicals can be done using visible or UV light, even for very low vibrational frequency modes, which cannot be accessed by infrared spectroscopy because of the lack of suitable infrared light sources. Second, the vibrationally cold anions greatly simplify the spectral congestions and even allow rotational profiles to be obtained for

complex species. Third, no van der Waals complexes are needed; as long as the neutral radical has a sufficiently large dipole moment to support dipole-bound states, its vibrational spectroscopy can be probed using the current technique.

[1] P. F. Bernath, *Annu. Rev. Phys. Chem.* **1990**, *41*, 91.
[2] E. Hirota, *J. Phys. Chem.* **1983**, *87*, 3375.
[3] M. E. Jacox, *Chem. Soc. Rev.* **2002**, *31*, 108.
[4] Y. Gong, M. F. Zhou, L. Andrews, *Chem. Rev.* **2009**, *109*, 6765.
[5] R. J. Saykally, *Science* **1988**, *239*, 157.
[6] S. K. Stephenson, R. J. Saykally, *Chem. Rev.* **2005**, *105*, 3220.
[7] S. S. Brown, *Chem. Rev.* **2003**, *103*, 5219.
[8] S. M. Ball, R. L. Jones, *Chem. Rev.* **2003**, *103*, 5239.
[9] T. Baer, R. C. Dunbar, *J. Am. Soc. Mass Spectrom.* **2010**, *21*, 681.
[10] W. H. Robertson, M. A. Johnson, *Annu. Rev. Phys. Chem.* **2003**, *54*, 173.
[11] M. Okumura, L. I. Yeh, J. D. Myers, Y. T. Lee, *J. Chem. Phys.* **1986**, *85*, 2328.
[12] M. A. Duncan, *J. Phys. Chem. A* **2012**, *116*, 11477.
[13] E. J. Bieske, O. Dopfer, *Chem. Rev.* **2000**, *100*, 3963.
[14] N. S. Nagornova, T. R. Rizzo, O. V. Boyarkin, *Angew. Chem.* **2013**, *125*, 6118; *Angew. Chem. Int. Ed.* **2013**, *52*, 6002.
[15] A. Fielicke, J. T. Lyon, M. Haertelt, G. Meijer, P. Claes, J. de Haeck, P. Lievens, *J. Chem. Phys.* **2009**, *131*, 171105.
[16] C. Romanescu, D. J. Harding, A. Fielicke, L. S. Wang, *J. Chem. Phys.* **2012**, *137*, 014317.
[17] E. L. Derro, C. Murray, T. D. Sechler, M. I. Lester, *J. Phys. Chem. A* **2007**, *111*, 11592.
[18] D. M. Wetzel, J. I. Brauman, *Chem. Rev.* **1987**, *87*, 607.
[19] U. Hefter, R. D. Mead, P. A. Schulz, W. C. Lineberger, *Phys. Rev. A* **1983**, *28*, 1429.
[20] W. C. Lineberger, T. A. Patterson, *Chem. Phys. Lett.* **1972**, *13*, 40.
[21] P. L. Jones, R. D. Mead, B. E. Kohler, S. D. Rosner, W. C. Lineberger, *J. Chem. Phys.* **1980**, *73*, 4419.
[22] D. M. Neumark, K. R. Lykke, T. Andersen, W. C. Lineberger, *J. Chem. Phys.* **1985**, *83*, 4364.
[23] B. M. Elliott, L. R. McCunn, M. A. Johnson, *Chem. Phys. Lett.* **2008**, *467*, 32.
[24] H. Schneider, K. M. Vogelhuber, F. Schinle, J. F. Stanton, J. M. Weber, *J. Phys. Chem. A* **2008**, *112*, 7498.
[25] C. L. Adams, H. Schneider, J. M. Weber, *J. Phys. Chem. A* **2010**, *114*, 4017.
[26] A. H. Zimmerman, J. I. Brauman, *J. Chem. Phys.* **1977**, *66*, 5823.
[27] R. L. Jackson, P. C. Hiberty, J. I. Brauman, *J. Chem. Phys.* **1981**, *74*, 3705.
[28] K. R. Lykke, D. M. Neumark, T. Andersen, V. J. Trapa, W. C. Lineberger, *J. Chem. Phys.* **1987**, *87*, 6842.
[29] D. M. Wetzel, J. I. Brauman, *J. Chem. Phys.* **1989**, *90*, 68.
[30] A. S. Mullin, K. K. Murray, C. P. Schulz, D. M. Szaflarski, W. C. Lineberger, *Chem. Phys.* **1992**, *166*, 207.
[31] K. Yokoyama, G. W. Leach, J. B. Kim, W. C. Lineberger, *J. Chem. Phys.* **1996**, *105*, 10696.
[32] K. Yokoyama, G. W. Leach, J. B. Kim, W. C. Lineberger, A. I. Boldyrev, M. Gutowski, *J. Chem. Phys.* **1996**, *105*, 10706.
[33] X. B. Wang, L. S. Wang, *Rev. Sci. Instrum.* **2008**, *79*, 073108.
[34] X. B. Wang, H. K. Woo, B. Kiran, L. S. Wang, *Angew. Chem.* **2005**, *117*, 5048; *Angew. Chem. Int. Ed.* **2005**, *44*, 4968.
[35] X. B. Wang, H. K. Woo, L. S. Wang, *J. Chem. Phys.* **2005**, *123*, 051106.

[36] P. D. Dau, H. T. Liu, D. L. Huang, L. S. Wang, *J. Chem. Phys.* **2012**, *137*, 116101.

[37] I. León, Z. Yang, L. S. Wang, *J. Chem. Phys.* **2013**, *138*, 184304.

[38] Z. Yang, I. Leon, L. S. Wang, *J. Chem. Phys.* **2013**, *139*, 021106.

[39] H. T. Liu, C. G. Ning, D. L. Huang, P. D. Dau, L. S. Wang, *Angew. Chem.* **2013**, *125*, 9146; *Angew. Chem. Int. Ed.* **2013**, *52*, 8976.

[40] J. D. Gu, J. Leszczynski, H. F. Schaefer, *Chem. Rev.* **2012**, *112*, 5603.

[41] I. Baccarelli, I. Bald, F. A. Gianturco, E. Illenberger, J. Kopyra, *Phys. Rep.* **2011**, *508*, 1.

[42] M. A. Yandell, S. B. King, D. M. Neumark, *J. Am. Chem. Soc.* **2013**, *135*, 2128.

[43] J. H. Hendricks, S. A. Lyapustina, H. L. deClercq, J. T. Snodgrass, K. H. Bowen, *J. Chem. Phys.* **1996**, *104*, 7788.

[44] J. Schiedt, R. Weinkauf, D. M. Neumark, E. W. Schlag, *Chem. Phys.* **1998**, *239*, 511.

[45] C. Desfrancois, H. AbdoulCarime, J. P. Schermann, *J. Chem. Phys.* **1996**, *104*, 7792.

[46] G. Hanel, B. Gstir, S. Denifl, P. Scheier, M. Probst, B. Farizon, M. Farizon, E. Illenberger, T. D. Mark, *Phys. Rev. Lett.* **2003**, *90*, 188104.

[47] X. F. Li, L. Sanche, M. D. Sevilla, *J. Phys. Chem. B* **2004**, *108*, 5472.

[48] E. C. M. Chen, J. R. Wiley, E. S. Chen, *Nucleosides Nucleotides Nucleic Acids* **2008**, *27*, 506.

[49] L. S. Wang, C. F. Ding, X. B. Wang, S. E. Barlow, *Rev. Sci. Instrum.* **1999**, *70*, 1957.

[50] H. T. Liu, Y. L. Wang, X. G. Xiong, P. D. Dau, Z. A. Piazza, D. L. Huang, C. Q. Xu, J. Li, L. S. Wang, *Chem. Sci.* **2012**, *3*, 3286.

[51] R. S. Berry, *J. Chem. Phys.* **1966**, *45*, 1228.

[52] J. Simons, *J. Am. Chem. Soc.* **1981**, *103*, 3971.

[53] P. K. Acharya, R. A. Kendall, J. Simons, *J. Am. Chem. Soc.* **1984**, *106*, 3402.

[54] Gaussian 09 (Revision A.02), M. J. Frisch, et al., Gaussian, Inc., Wallingford CT, **2009**. (please see ref. [S6] of the Supporting Information for the full authors list).

[55] R. Krishnan, J. S. Binkley, R. Seeger, J. A. Pople, *J. Chem. Phys.* **1980**, *72*, 650.

[56] C. T. Lee, W. T. Yang, R. G. Parr, *Phys. Rev. B* **1988**, *37*, 785.

[57] A. D. Becke, *J. Chem. Phys.* **1993**, *98*, 5648.

[58] M. A. Kurinovich, J. K. Lee, *J. Am. Chem. Soc.* **2000**, *122*, 6258.

[59] B. F. Parsons, S. M. Sheehan, T. A. Yen, D. M. Neumark, N. Wehres, R. Weinkauf, *Phys. Chem. Chem. Phys.* **2007**, *9*, 3291.

[60] C. M. Western. PGOPHER, a Program for Simulating Rotational Structure, University of Bristol, http://pgopher.chm.bris.ac.uk.

2468   www.angewandte.org

© 2014 Wiley-VCH Verlag GmbH & Co. KGaA, Weinheim

Angew. Chem. Int. Ed. **2014**, *53*, 2464–2468